Rational Simplification of High Fidelity Wind Turbine Models Used for Mooring Analysis

Rational Simplification of High Fidelity Wind Turbine Models Used for Mooring Analysis

Marit I Kvittem[1], Arnt G Fredriksen[2], Carlos S de Souza[1], and Finn-Christian W Hanssen[3]

[1] SINTEF Ocean, Trondheim, Norway, [2] Entail, Oslo, Norway, [3] Semar, Oslo, Norway

E-mail: marit.kvittem@sintef.no

Abstract. This study investigates the use of simplified turbine modelling in analysis of a soft mooring system (horizontal plane periods > 250 s). Two simplified turbine models are developed, tested and compared to a high fidelity turbine model in a case study of the INO WINDMOOR 12 MW FOWT with a soft mooring system. The chosen simplified modelling strategies are a drag disc model, a de-coupled approach where the aerodynamic loads are pre-calculated in a fixed turbine simulation and a model with reduced degrees-of-freedom. Corrections to the pre-calculated force model is also developed and compared. The results show that the pre-calculated force approach gives better comparisons to the full model than the drag disc model, and that applying a controller correction to account for the wind turbine controller's response to floater motions improves the predicted response.

1. Introduction

The floating wind market is rapidly expanding, with many floating wind farms planned worldwide. To bridge the cost gap between floating and bottom-fixed wind, developers consider shared mooring systems such as the innovative Honeymooring solution by Semar (Figure 1) as a promising technology. Such systems introduce mechanical couplings between the floating units, and thus poses new challenges for mooring analyses. Advanced coupled aero-, hydro-, servo-elastic models for single units have been established over the last two decades, and they have even been applied for multiple coupled turbines using HAWC2Farm [1] and OpenFAST [2] (using co-simulation of individual models). However, such high-fidelity models may be impractical to use in a farm with coupled units since 1) they are computationally heavy and 2) representing a turbulent wind field over the size of a wind farm requires storage of large data quantities.

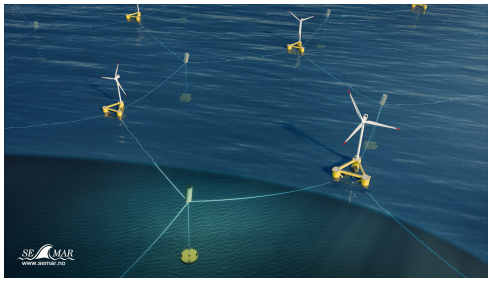

Figure 1: HoneyMooring.

Through increased computational efficiency, simplified turbine models could represent a useful modelling strategy for systems with multiple turbines. Several authors have previously adopted simplified turbine models successfully, e.g. using pre-calculated (de-coupled) aerodynamic forces for a bottom fixed offshore wind turbine in time domain (Chen

Ong et al. [3]) or frequency domain approaches (De Souza et al. [4], Pegalajar et al. [5], Lupton [6], Kvittem and Moan [7] and Bachynski [8]).

To understand the utility of simplified turbine models, it is crucial to assess their accuracy. The present paper evaluates several simplified models to represent aerodynamic loads on floating offshore wind turbines (FOWT) in time domain that can be implemented in commercial software (like SIMA and OrcaFlex). The aim of the models is to accurately represent the behavior of the mooring system with improved computational efficiency, thus guiding the way towards practical engineering tools for coupled wind farm design.

This paper describes three different simplified modelling strategies using a drag disc model, pre-calculated aerodynamic forces (with or without controller-induced damping) and degree-of-freedom-reduction. The models are compared with a fully coupled aero-, servo-elastic model.

2. Turbine Models

This section describes the principles of simplified modelling applied in this study, in addition to introducing the high fidelity benchmark turbine model. The drag disk model and the pre-calculated force model use the same finite element- and multi-body model, where the turbine model is replaced by its contribution to mass and gravity, in addition to rotor loads and tower drag.

When the term *high fidelity model* is used in this paper, it refers to an aero-, hydro-, servo-elastic beam model of the wind turbine, as is state-of-the-art for turbine foundation design analysis. Models with higher fidelity exist (e.g. 2D elements for the blades, computational fluid dynamics models or vortex method aerodynamics), but this is not what is meant here.

2.1. High Fidelity Turbine Model

The high fidelity turbine (also called *Full turbine model*) is modeled using beam-column elements with aerodynamic loads according to Blade Element Momentum (BEM) theory for the blades. Rotor speed and blade pitch are controlled by a wind turbine controller. Spatial turbulence variation is represented by a turbulence box pre-generated using the Mann model [9], and wind speed is sampled at the instantaneous position of the blade elements.

The tower is modelled using beam-column elements with wind loads accounted for through quadratic drag. The SIMA BEM implementation includes unsteady aerodynamics by using dynamic inflow correction and dynamic stall. Tower shadow is included using a potential flow theory [10].

2.2. Drag Disk Model

The aerodynamic force in the axial direction as a function of time ($T(t)$) is represented using variable quadratic thrust coefficients ($C_T(U_{mean})$) at the hub position according to Eq. 1, where $U_{hub}^{rel}(t)$ is the incident relative velocity at the hub sampled from the same turbulence box as in the full turbine model.

$$T(t) = C_T(U_{mean}) * U_{hub}^{rel}(t)^2 \tag{1}$$

Thrust coefficients representing different mean wind speeds (U_{mean}) are calculated based on the aerodynamic axial rotor force from steady-wind simulations (with wind shear) using the high fidelity model fixed at the tower base.

The drag coefficient approach gives a model that takes into account the relative, turbulent, wind velocity at the hub, which to some degree accounts for both turbulence and floater motion. However, the rotational sampling of spatial turbulence is not included, and neither is the interaction with the wind turbine controller. Additionally, the approach only gives axial aerodynamic forces, i.e., neglects aerodynamic loads in the other DOFs.

2.3. Pre-calculated Aerodynamic Loads
As for the drag model, a high fidelity model of the turbine fixed at the tower base is used to extract the aerodynamic loads. In this approach, the same turbulent wind field as in the high fidelity turbine analysis is applied, and six DOF aerodynamic loads are extracted and stored as timeseries. These are subsequently applied directly to the hub in an analysis with a floating platform.

Unlike in the drag model, using pre-calculated loads accounts for the rotational sampling of spatial turbulence, controller response to turbulence, and for aerodynamic loads in all six DOF. The pre-calculated loads approach does, however, not include the effects of the controller's response to the actual *relative* wind speed that the turbine sees due to the platform motion. To account for this in the floater model, the correction described in Section 2.3.1 is introduced.

2.3.1. Controller Correction It is well known that the controller interacts with the floater motions of FOWTs [11], which is why the controller gains are modified compared to a fixed wind turbine. De Souza and Bachynski [12] showed that below rated wind speeds (where there is no feedback control of the blade pitch angle), the rotor thrust provides *positive* damping to the motions. Above the rated wind speed, the sign and magnitude of the damping depend on the controller natural frequency, relative to the floater motions. A de-tuned controller is normally meant to have a natural frequency lying between the platform's surge and pitch natural frequencies. As a result, the damping induced by the rotor will be positive for the pitch motions, but still *negative* for the surge motions.

To account for the additional positive or negative damping, a controller correction application has been developed, using a Dynamic-link Library (DLL). The correction assumes a rotor linearized around the mean wind speed (operation point), and calculates the additional change in thrust force due to the nacelle/hub velocity. Eqs. 2 & 3 are the basic equations for the change in aerodynamic torque ΔQ_a and thrust ΔT, respectively. The theory behind this is similar to that presented by De Souza et. al. [4], but the application here is time domain analysis.

$$\Delta Q_a = \Delta\Omega \frac{\partial Q}{\partial \Omega} + \Delta u \frac{\partial Q}{\partial u} + \Delta\beta \frac{\partial Q}{\partial \beta}, \tag{2}$$

$$\Delta T = \Delta\Omega \frac{\partial T}{\partial \Omega} + \Delta u \frac{\partial T}{\partial u} + \Delta\beta \frac{\partial T}{\partial \beta}. \tag{3}$$

Here, $\Delta\Omega$ is the change in rotor speed, Δu is the change in wind velocity (which is the instantaneous hub velocity in this case), and $\Delta\beta$ is the change in blade pitch angle. The derivatives are obtained with the linearization module of OpenFAST for each operational point, associated with a list of wind speeds, and then interpolated at the relevant mean wind speed to be used in a given simulation. Δu is passed every timestep to the DLL, whereas $\Delta\Omega$ and $\Delta\beta$ are found by solving a state space system, and depend on the controller regime. In this study, we simplify controller regimes as *below rated* and *above rated* only.

The error in rotation speed, $\Delta\Omega$, is taken as the difference between the actual (measured) rotor speed and the reference rotor speed. In a variable speed generator, like the WINDMOOR 12 MW turbine, the reference rotor speed varies below rated wind speed with the blade pitch angle kept at zero. Above rated, the rotor speed is kept constant, and the blade pitch is changed to modify the aerodynamic torque.

$$I_d \dot{\Omega} = \Delta Q \tag{4}$$

where I_d is the rotor inertia and $\dot{\Omega}$ is the rotor acceleration.

In the FOWT analysis, the controller correction force is applied by calling an external DLL in SIMO, which again calls a Python library that contains functions to calculate the change in thrust force.

Below Rated Wind Speed

Below rated wind speed, the rotor speed is controlled to obtain optimal power production with blade pitch kept constant ($\Delta\beta = 0$). The reference rotor speed is taken as a function of mean wind speed. To find the necessary change in generator torque, ΔQ, to correct the rotor speed, Eq. 4 is solved directly using Euler integration.

Above Rated Wind Speed

Above rated wind speed, the controller is set to operate at a reference rotation speed, Ω_r, and the blade pitch angle is used to regulate the aerodynamic torque. The proportional-integral (PI) controller used in this study, uses the following connection between blade pitch change ($\Delta\beta$) and rotor speed:

$$\Delta\beta = K_p\Delta\Omega + K_i \int_0^t \Delta\Omega \, dt. \tag{5}$$

Here, K_p and K_i are coefficients tuned for the system. Equations 4 and 5 are solved using a state-space formulation. The INO WINDMOOR 12 MW controller uses gain scheduling, and the gain tables are given in the input file to the DLL.

Equation 4 is valid also for above rated conditions, which together with Eq. 5 gives two differential equations that are solved using a state-space formulation. The remaining ordinary differential equation is solved using Euler integration.

The rated condition represents a transitional controller region which is not easily linearized. However, since it gives a fair comparison with the high fidelity model, the approach with pre-calculated loads without any correction is applied for the rated case (LC3) in this study.

2.3.2. Yaw Inflow Effect Wind turbine rotor forces cause moments around the vertical axis of the turbine foundation, since the rotor centre is eccentric to the foundation. The larger the distance between the hub and the foundation centre, the larger the moment arm. This contributes with righting (e.g. for the 0° case) or driving (e.g. for the 180° case) yaw moments on a floating foundation. For the INO WINDMOOR 12 MW, which is a three-column semi-submersible with eccentric tower, this has proven to cause large yaw rotations in certain combinations of wind speed and wind direction.

Two physical effects related to aerodynamic yaw moments are observed:

- *Self-enhancing yaw moments*: Platform yaw changes the yaw inflow angle, which increases the aerodynamic forces that contribute to platform yaw, until equilibrium is reached. This is considered to be a quasi-static problem.
- *Fishtailing behaviour*: Platform yaw alternates between two marginally stable equilibrium positions. This behaviour is observed in dynamic analyses, but in essence the same as the self-enhancing yaw moments.

2.4. Degree-of-Freedom Reduction

Another approach includes a full turbine model established in simulation software OrcaFlex, which has a feature to reduce the degrees of freedom by considering the blades as rigid. With the blades considered stiff, the local deformation of the blades is disregarded, which is expected to reduce the computational time.

2.5. Comparison of Models

An illustration of how the models explained above work is given in Fig. 2, together with an overview of the physical effects accounted for (Tab. 2d). Note that the tower is considered as stiff in models in Figs. 2b and 2c, but with the same aerodynamic drag coefficients as the full turbine in Fig 2a. The different models described above can be summarized as follows:

A) Full turbine model with rigid blades (reduced no. of DOFs)
B) Drag model
C) Pre-calculated aerodynamic loads
D) Pre-calculated aerodynamic loads + controller correction.

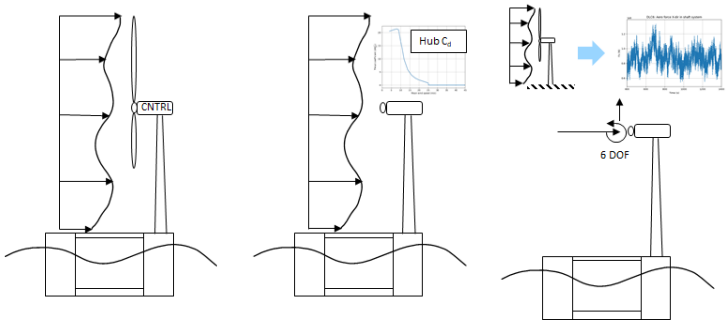

(a) A (b) B (c) C&D

Effect/Model	A	B	C	D
Turbulent wind	X	X	X	X
Tower drag	X	X	X	X
Rotational sampling	X	0	X	X
Control - turbulence	X	0	X	X
Control - floater motion	X	0	0	X
Wind inflow misalign.	X	0	0	0
Flexible blades	*	0	*	*
Flexible tower	X	0	0	0
Gyroscopic effect	X	0	0	0

(d) X - included, 0 - not included, * - effect partly included.

Figure 2: Illustration of model principles and summary of differences between effects included in the models.

3. Case Study

3.1. Wind Turbine

The INO WINDMOOR 12 MW wind turbine [13] is used for comparing the models . This is a 12 MW wind turbine supported by a three-column semi-submersible foundation. The base case described in [13] is anchored with a semi-taut system of three lines. The platform used here includes mean wave drift loads and damping calibrated against model tests as described in [14] (additional sea-state dependent linear and quadratic surge- and sway damping coefficients are listed in Tab. 2).

The current study considers a mooring system established to better represent the soft behaviour of the HoneyMooring system illustrated in Fig. 1. The surge-, sway and yaw resonance periods (at rest) are 266.7 s, 265.2 s and 258.7 s, respectively.

The WINDMOOR 12 MW turbine uses the PI-control from the ROSCO controller to control the torque and blade pitch, with controller gains tuned specifically for this platform to minimize negative floater pitch-motion damping. More detailed specifications of the turbine and floater can be found in [13].

3.2. Mooring System

The FOWT is connected with polyester mooring lines from the fairleads to three buoys, which again are connected to the seabed with taut polyester lines. The fairleads, buoys and anchors have a spread angle of 120°. The fairlead- and buoy radius with respect to the platform centre is 42.7 m and 786.4 m, respectively, and the respective vertical positions are at the sea surface and at 48.7 m water depth. The anchors have the same x- and y coordinates as the buoys, and are located at the seabed (150 m). Mooring line properties are listed in Tab. 1. Each of the buoys are modelled as 52 t nodal masses with a volume of 325 m^3. In axial direction, the drag and added mass coefficients are 1.1 and 0.13, respectively. Corresponding values in transverse direction are 0.9 and 0.83.

Table 1: Mooring line data.

Component	Line length (m)	Mass (kg/m)	Ext. area (m^2)	Axial stf. (N)	Stf. damping $(-)$	CQ_x/CQ_y $(-)$	CA_x/CA_y $(-)$
Fairlead - Buoy	744.40	16.80	4.62	1.81E8	0.01	0.008/1.400	0.0/1.0
Buoy - Anchor	101.30	34.50	6.63	3.46E8	0.01	0.008/1.400	0.0/1.0

3.3. Environmental Conditions

The water depth used in this study is 150 m, the gravitational acceleration constant is 9.81 m/s^2 and the seawater density is 1025 kg/m^3. Representative environmental conditions were selected from a met-ocean report for a site in Eastern Asia, and are listed in Tab. 2. The selected wind speeds represent different states of the turbine (cut-in, below rated, rated, above rated, cut-out and idling), together with conditional sea-state parameters.

Table 2: Environmental conditions and sea-state dependent damping coefficients.

LC #	State	U_{mean} (m/s)	Turb. mod.	α (-)	Hs (m)	Tp (s)	$B1_{lin}$ (Ns/m)	$B2_{lin}$ (Ns/m)	$B1_{quad}$ (Ns^2/m^2)	$B2_{quad}$ (Ns^2/m^2)
1	oper.	4	NTM	0.065	0.8	6.4	5.242E3	4.840E3	0	0
2	oper.	8	NTM	0.065	1.2	6.9	1.027E4	9.898E3	0	0
3	oper.	10.6	NTM	0.065	1.5	7.4	1.401E4	1.400E4	0	0
4	oper.	12	NTM	0.065	1.6	7.5	1.552E4	1.561E4	0	0
5	oper.	14	NTM	0.065	2.0	7.9	2.184E4	2.244E4	0	0
6	oper.	17	NTM	0.065	2.5	8.3	3.084E4	3.218E4	6.148E4	6.148E4
7	oper.	23	NTM	0.065	4.2	9.5	6.194E4	6.536E4	9.838E4	9.838E4
8	idling	38	EWM	0.09	9.8	10.8	1.805E5	1.854E5	2.578E5	2.578E5
9	idling	46	EWM	0.09	11.8	11.7	1.901E5	1.987E5	3.902E5	3.902E5

Since direct comparison between models is carried out, a single three-hour realization after a 400 s transient phase is carried out for each case with the same random seed for wind and waves for each model. In line with IEC-61400-3-2 [15], 600 s long turbulence time series was repeated. Please note this may cause unphysical resonant behavior in systems with long natural periods, however, this will be the case for all model variations compared.

3.4. Simulation Software

While the comparison of the drag disk model and the pre-calculated force model are carried out using a SIMA, comparison of the reduced DOF model is done with OrcaFlex. The reason for this is the available features in the different software packages. In both cases, the simplified models are compared to high fidelity turbine benchmarks.

4. Results

4.1. Reduced Degree-of-Freedom Model

Two approaches are compared here: In the first, the shape and twist of the blades is taken as the initial non-deformed shape, and as shown by Fig. 3, this result in somewhat lower thrust around rated speed. In the other approach, the quasi-static deformed shape of the blades including twist is extracted, and enforced as blade deformation in constant wind simulation with all DOF included. This results in a thrust similar to the deformed case.

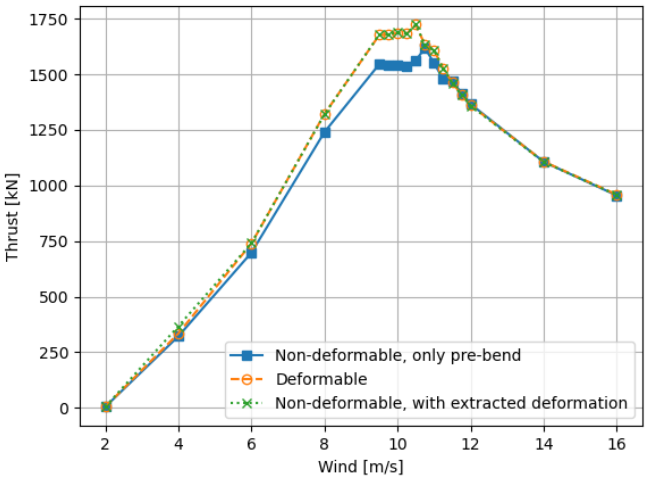

Figure 3: Thrust curve in constant wind using deformable and non-deformable blades

4.2. Drag Disc Model and Pre-calculated Loads Model

Fig. 4 shows mean and standard deviations for line tensions at fairlead and platform motions for environment directions 0°. Mean values for motion in line with the wind direction (surge and pitch) obtained using both the drag disc model and the model with pre-calculated loads generally agree well with the full turbine reference case. The same trend is observed for the mean mooring line tensions.

The drag disc model predicts close to zero motion perpendicular to the wind direction (sway and roll), which is natural since there are no aerodynamic coefficients in other directions than the shaft direction. The pre-calculated loads model uses aerodynamic excitation in six DOF, which better represents mean motions in sway and roll. Except for LC7, the pre-calculated loads model also predicts mean yaw motions with good accuracy.

Fig. 4 shows that both simplified models predict standard deviations for surge and pitch motions well in the parked conditions (LC8 and LC9), but with notable differences for the operational cases (LC1-LC7). The drag disc model and the pre-calculated force model both over- and under-predict the surge and pitch motion compared to the full turbine reference case. Where the drag model mostly over-predicts the surge- and pitch response, the pre-calculated force model over-predicts the response below rated wind speed, and under-predicts above rated wind speed. Using the controller correction DLL (as described in Section 2.3.1), improves the prediction of surge and pitch standard deviations.

By studying Fig. 5, the magnitude of the resonant peak in the surge spectra (around 0.003-0.005 Hz, depending on the wind speed) differs between the models. This suggests that damping is the main source of difference between the models. Adding the controller correction DLL significantly improves the accuracy compared to the full turbine model, in particular for below

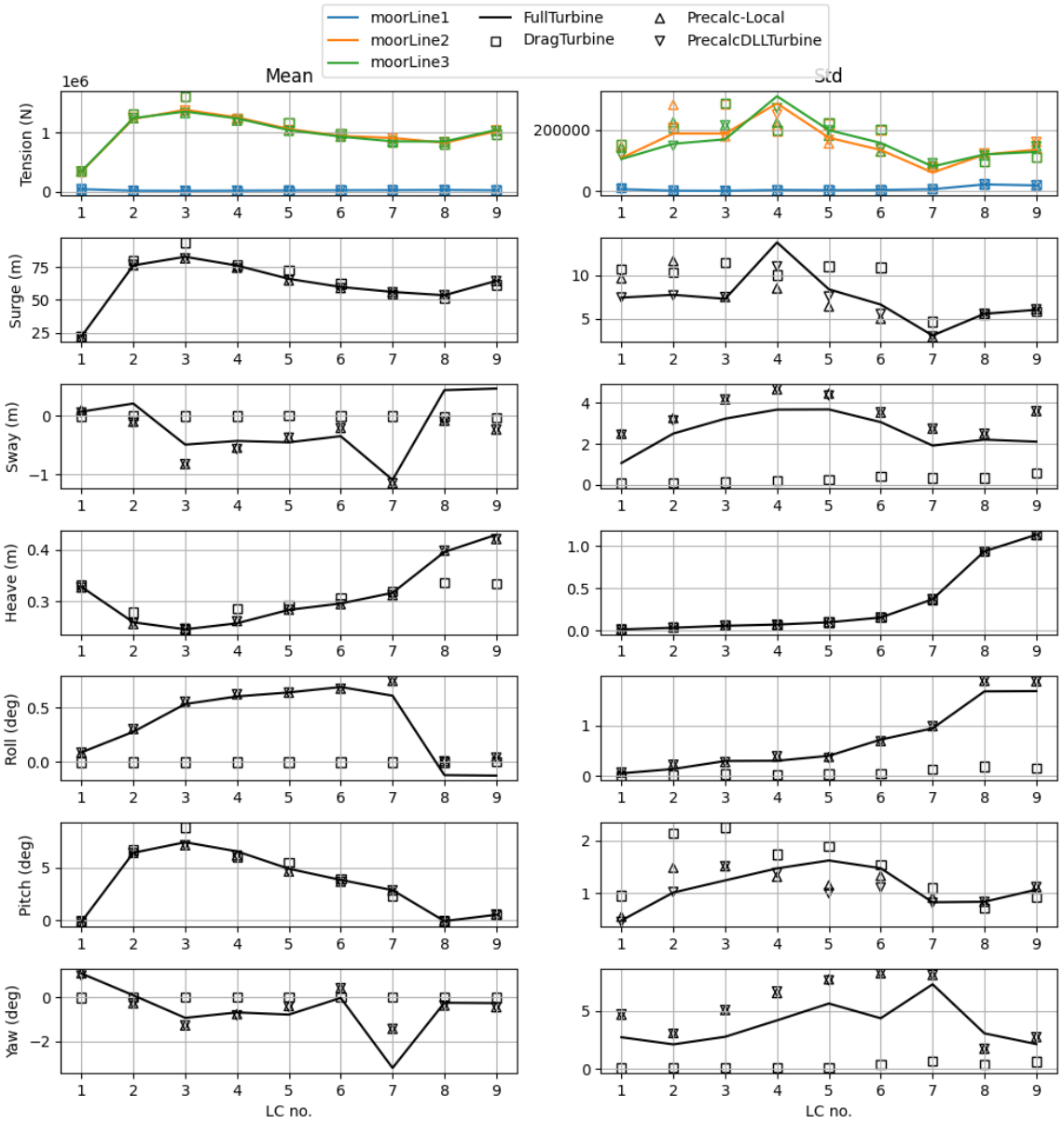

Figure 4: Statistics - environment from 0°

rated cases (LC1-LC2). The correction assumes a linearized rotor, which could explain the lesser improvement for above rated cases.

Mooring line tensions at fairlead (statistics in Fig. 4 and spectra in Fig. 5) are strongly related to the low frequency surge and sway motion. Low frequency sway motion (resonance frequency around 0.008 Hz) is over-estimated by the simplified models, and since the DLL only corrects the thrust force, no improvement of the pre-calculated model is seen in this context. Nevertheless, the response spectra in Fig. 5 clearly show that the low frequency distribution is much better represented by applying a pre-calculated force than using a calibrated one degree of freedom drag model.

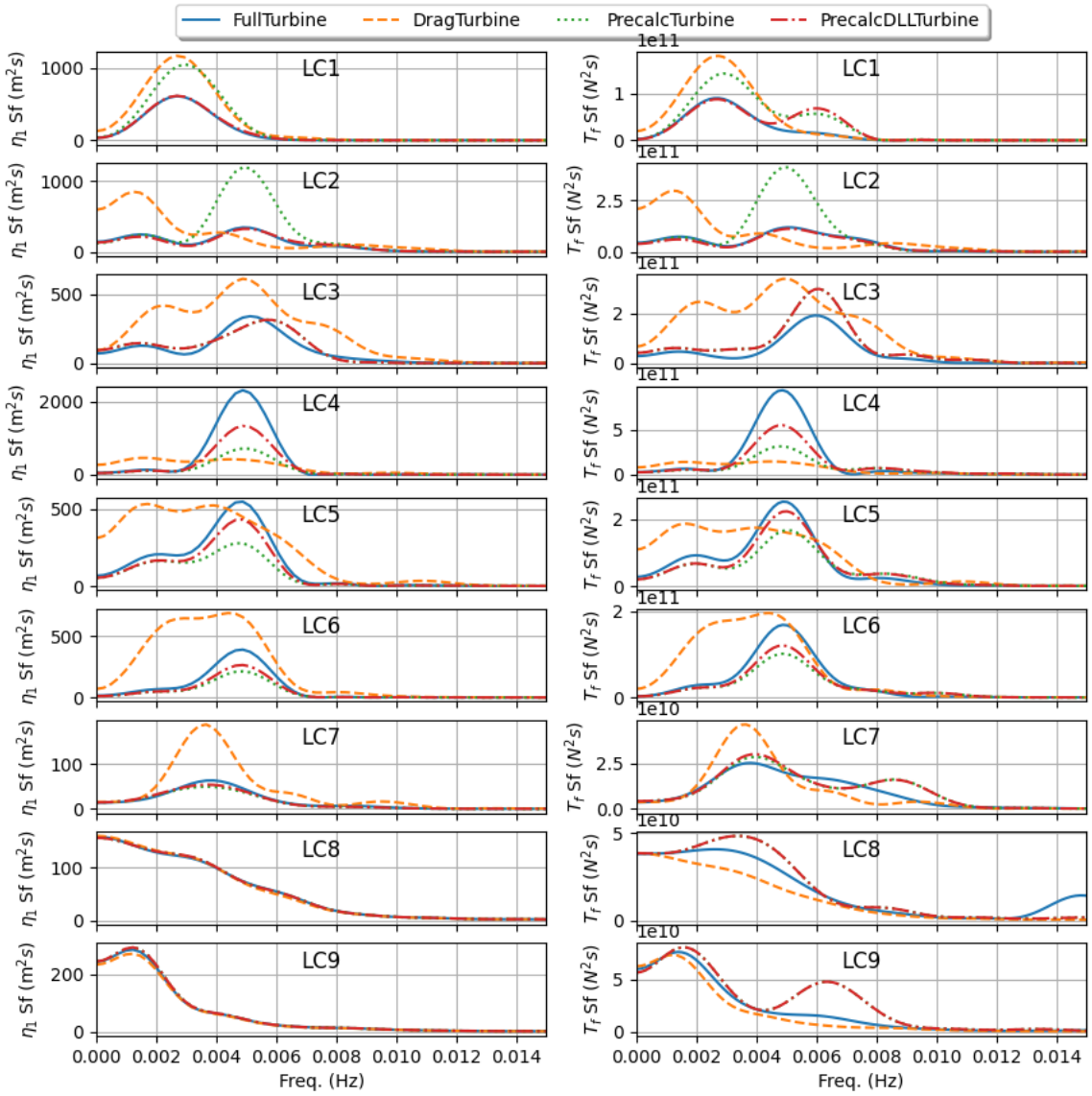

Figure 5: Spectral density for surge (η_1) and fairlead tension (T_f) - environment from 0°

4.2.1. 180° Wind Direction and Yaw Motions This paper only presents results for when the wind comes from 0°. Simulations and comparisons are also performed for 180° environment direction, which gives similar conclusions. However, there are three load cases that seem to encounter yaw motion challenges for wind coming in at 180° - LC7, LC8 and LC9. In LC7 (operation), one can observe fishtailing behaviour, where the platform seems to alternate between two quasi-static equilibrium points. In LC8 and LC9 (idling), large yaw motions are observed. The reason why this occurs at 180° is that yaw moments caused by aerodynamic rotor forces are driving for this wind direction, as explained in Sec. 2.3.2. The simplified models presented

in this paper failed to represent unstable yaw behaviour.

5. Conclusions

In this study, simplified turbine models are developed, tested and compared to a high fidelity turbine model in a case study of the INO WINDMOOR 12 MW FOWT with a soft mooring system. The chosen simplified modelling strategies are a drag disc model and a de-coupled approach where the aerodynamic loads are pre-calculated in a fixed turbine simulation before it is applied to a floating turbine model. A correction to the pre-calculated force approach is also included, accounting for the interaction between the floating motion and the wind turbine controller. A model with reduced DOFs was also evaluated, with good results for the case where a deformed blade configuration was assumed.

The simplified models gave a 45% reduction in simulation time, compared to the reference case. For approach the approach with reduced DOFs, there was no reduction in the computational time due to issues with the implementation of this functionality in OrcaFlex. However, in principle, this approach should result in reduced computational time.

Overall, the pre-calculated force model gives better comparisons to the full model than the drag disc model - estimates of mean and standard deviation are better and the response spectra show a more similar frequency content. The surge- and pitch frequency resonant response is over-predicted in below rated conditions and under-predicted in above-rated conditions. Adding a linearized controller correction, that applies a change in thrust force due to a change in hub velocity, gives improved results, particularly for below-rated conditions.

For wind speeds close to cut-out, and in the idling conditions, when wind comes from 180°, turbine forces give a driving yaw moment. It is thus recommended that simplified models applied in cases with both high wind speed and a wind direction causing driving yaw moments, include a representation of the non-linear aerodynamic effect that drives the unstable yaw behaviour.

Acknowledgments

The work is part of the HoneyMooring R&D project, funded by the Research Council of Norway through the ENERGIX programme (grant 321593), and industry partners. The preparation of this paper was partly funded by the WINDMOOR project, also funded by the Research Council of Norway through the ENERGIX programme (grant 294573).

References

[1] Gözcü O, Kontos S and Bredmose H 2022 *Journal of Physics: Conference Series* **2265** 042026 ISSN 1742-6596 URL https://doi.org/10.1088/1742-6596/2265/4/042026

[2] Hall M and Connolly P 2018 Coupled dynamics modelling of a floating wind farm with shared mooring lines *International Conference on Offshore Mechanics and Arctic Engineering* URL https://doi.org/10.1115/OMAE2018-78489

[3] Chen Ong M, Bachynski E E and David Økland O 2017 *Journal of Offshore Mechanics and Arctic Engineering* **139** ISSN 0892-7219 URL https://doi.org/10.1115/1.4035772

[4] Souza C E S, Hegseth J M and Bachynski E E 2020 *Journal of Physics: Conference Series* **1452** 012040 ISSN 1742-6596 URL https://dx.doi.org/10.1088/1742-6596/1452/1/012040

[5] Pegalajar-Jurado A, Borg M and Bredmose H 2018 *Wind Energy Science* **3** 693–712 ISSN 2366-7443 URL https://doi.org/10.5194/wes-3-693-2018

[6] Lupton R C 2015 *Frequency-domain modelling of floating wind turbines* Doctoral thesis University of Cambridge URL https://doi.org/10.17863/CAM.14119

[7] Kvittem M I and Moan T 2014 *Journal of Offshore Mechanics and Arctic Engineering* **137** ISSN 0892-7219 URL https://doi.org/10.1115/1.4028340

[8] Bachynski E E 2014 *Design and Dynamic Analysis of Tension Leg Platform Wind Turbines* Doctoral thesis Norwegian University of Science and Technology URL http://hdl.handle.net/11250/238768

[9] Mann J 1998 *Probabilistic Engineering Mechanics* **13** 269–282 ISSN 0266-8920 URL https://doi.org/10.1016/S0266-8920(97)00036-2

[10] SINTEF Ocean 2023 *RIFLEX Theory Manual* URL https://sima.sintef.no/doc/4.4.0/userguide/index.html
[11] Larsen T J and Hanson T D 2007 *Journal of Physics: Conference Series* **75** 012073 ISSN 1742-6596 URL https://doi.org/10.1088/1742-6596/75/1/012073
[12] Souza C E S and Bachynski E E 2019 *Ocean Engineering* **180** 223–237 ISSN 0029-8018 URL https://doi.org/10.1016/j.oceaneng.2019.02.075
[13] Silva de Souza C E, Berthelsen P A, Eliassen L, Bachynski E E, Engebretsen E and Haslum H 2021 *Definition of the INO WINDMOOR 12 MW base case floating wind turbine* (SINTEF Ocean) ISBN 978-82-7174-407-6 URL https://sintef.brage.unit.no/sintef-xmlui/handle/11250/2723188
[14] Silva de Souza C E, Fonseca N, Berthelsen P A and Thys M 2021 Calibration of a time-domain hydrodynamic model for a 12 MW semi-submersible floating wind turbine *International Conference on Offshore Mechanics and Arctic Engineering* URL https://doi.org/10.1115/OMAE2021-628575
[15] International Electrotechnical Commission 2019 IEC61400-3-2: Wind energy generation systems - part 3-2: Design requirements for floating offshore wind turbines